

# Some Physicochemical Properties of $\text{Yb}_{14}\text{MnSb}_{11}$ and Its Solid Solutions with Gadolinium $\text{Yb}_{14-x}\text{Gd}_x\text{MnSb}_{11}$ Type

Makhsuda Abdusalyamova<sup>1,a</sup> and Inga Vasilyeva<sup>2</sup>

<sup>1</sup>Institute of Chemistry named after V.I. Nikitin AS of Republic of Tajikistan, 299/2, Str. Aini, 734063, Dushanbe, Tajikistan

<sup>2</sup>Nikolaev Institute of Inorganic Chemistry, RAS, Siberian Branch, Lavrentiev Avenue, 3, 630090, Novosibirsk, Russia

**Abstract.** Data on structure, melting temperatures, density, thermal dilatation, kinetic of oxidation of  $\text{Yb}_{14}\text{MnSb}_{11}$  and its solid solutions with gadolinium are presented in this article. All solid solutions are isostructural with Zintl compound  $\text{Ca}_{14}\text{AlSb}_{11}$  and crystallizes in tetragonal structure. Investigations melting temperatures, thermal dilatation, oxidation have shown that Gd incorporation near  $\text{Gd} \approx 0.5$  and increased melting point and thermal dilatation.

## 1 Introduction

Zintl phases form a large family of compounds whose electronic conform to 8-N or Zintl – Klemm concept. This class of materials has been identified as promising for thermoelectric (TE) applications. A new direction of thermoelectric materials began when Slack theorized the so-called “electron crystals-phonon glass” [1]. Slack considered that a good TE material should have the electronic structure of a heavily doped narrow-band-gap semiconductor and thermal conductivity like a glass. One of new class materials for utilization as high-temperature thermoelectric materials are Zintl phases that employ the pnictides of rare earth elements and have the  $\text{Ca}_{14}\text{AlSb}_{11}$  structure type. For the first time Zintl phase of  $\text{Yb}_{14}\text{MnSb}_{11}$  was obtained in 1998 [2].  $\text{Yb}_{14}\text{MnSb}_{11}$  is high-temperature thermoelectric material [2-5].

Effectiveness of the material which is often used to convert thermal energy into electrical is characterized by coefficient  $zT$  ( $zT = S^2 T / \rho k$ ), where  $S$  - Zeebeck coefficient,  $\rho$  - electrical resistance,  $k$  - thermal conductivity). All these three parameters are interlinked and one is optimized at the expense of others. Solid solutions with lanthanum, cerium, thulium, lutetium (partial replacement of ytterbium) [6-11], with aluminum (replacement of manganese) [12], germanium, tellurium (partial replacement of antimony) [13,14] have been investigated with an aim towards increasing  $zT$ .

In spite of numerous publications, there are no works on thermal properties, there are no works on chemical properties. From the position of thermoelectric materials thermal stability of these materials is also functional property since the exploitation of the material is carried out under high temperatures, where diffusion, volatility, oxidation processes easily occur.

Due to this the results of melting temperature and thermal dilatation, kinetic of oxidation of  $\text{Yb}_{14}\text{MnSb}_{11}$  and its solid solutions with gadolinium are presented in the present work.

## 2 Experimental details

### 2.1 Synthesis

Crystals with the expected stoichiometry of  $\text{Yb}_{14-x}\text{Gd}_x\text{MnSb}_{11}$  were grown from a molten Sn flux ( $\text{Yb}_{14-x}\text{Gd}_x\text{Mn}_6\text{Sb}_{11}\text{Sn}_{86}$ ) in a glassy carbon crucible. The elements were divided into layers: antimony- manganese- Gd- ytterbium-tin and quartz cotton that plays the role of filter at centrifugation was placed above. The crucible was placed in quartz ampoule pump out and seal. Pumped out quartz ampoule is placed in to the furnace and heat up to  $1000^\circ\text{C}$  with the delay at this temperature for 6 hours. Cooling up to  $700^\circ\text{C}$  was made at rate  $2^\circ/\text{hour}$ . At  $700^\circ\text{C}$  ampoule was taken out from the furnace and centrifuged for 5 minutes. Crystals are separated into dry box [2].

### 2.2 Electron microprobe analysis

The samples analyzed using a Camera JXA-8100 (JEOL, Japan) Electron Probe Micro-analyzer equipped with a wavelength-dispersive spectrometer with 20 keV accelerating potential and 30 nA beam current. Net elemental intensities were determined with respect to calibration standards of  $\text{YbPO}_4$ ,  $\text{GdPO}_4$ ,  $\text{SnO}_2$ , Sb (high concentration relation to that in “14-1-11”), and Al-garnet-Arizona ruby O-145 (here content of MnO was 9.9 mass.%). The composition of the major phase in each sample was determined by calculating averages and standard deviations from 15-30 random data points. The

<sup>a</sup>MakhsudaAbdusalyamova: amakhsuda@mail.ru

composition of the minor phases was determined from 5-7 data points depending on the area of the phases and it was not sufficient for standard deviation (Table 1).

### 2.3 Powder X-ray diffraction

X-ray structural study of single samples was conducted on the apparatus DRON-UM (R=192mm, CuK $\alpha$ -radiation, Ni-filter, scintillation detector with amplitude discrimination, step 0.02° 2 $\theta$ , impulse storage time in each point 3 s, room temperature) in the region of angles from 5 to 80° 2 $\theta$ . Total shooting time was 9 hours. After crystal pounding in the mortar with heptanes and suspension drying on the polished side of the standard quartz cavity, the sample was flat and thin (~ 100  $\mu$ m) layer. All studied samples have tetragonal structure and obtained lattice parameters are given in the Table 2.

### 2.4 Thermal stability

Thermal analysis with 2-3 mg was repeated 3-5 times with each sample. Two procedures were developed to study thermal stability of the tested samples. First was heating with the rate of 3000°C/min up to 1900°C in apparatus with the He pressure equal to 7 atm. During heating, all variations with the sample were fixed and related to appropriating peaks on the heating curve. Second procedure was step-by-step heating with examination what happens with the sample being heated to a given temperature. Three temperatures were taken: up to 1500°C, then 1750°C and at last 1900°C to fix stability without any vaporization, melting, and incongruent evaporation of melt. The apparatus was calibrated by melting point of Pd (1554°C) used as standard and this action was performed before and after measurements of the sets of the samples.

### 2.5 Thermal expansion

Thermal expansion was measured in cylindrical samples about 4 mm in diameter, 10-13mm long the temperature range 25-750°C using a high-temperature dilatometer which construction is described in [15].

### 2.6 Kinetics

Oxidation kinetics was studied using thermogravimetric method based on the continuous sample weighing at temperatures 773, 873 и 973°C. Oxidation was carried out in air atmosphere in alumina crucibles.

## 3 Results and discussion

The experimental data were treated mathematically and the compositions of the major and minor phases and their calculated errors are given in Table 1.

The powder X-ray diffraction patterns for some samples are shown in Figure 1.

**Table 1.** Composition of the major and minor phases observed.

Yb <sub>13.9</sub> Gd <sub>0.1</sub> MnSb <sub>11</sub>	Yb <sub>13.88</sub> Gd <sub>0.17</sub> Mn <sub>1.13</sub> Sb <sub>11</sub> Yb <sub>13.90</sub> Gd <sub>0.17</sub> Mn <sub>1.13</sub> Sb <sub>11</sub>	Sn Sn
Yb <sub>13.7</sub> Gd <sub>0.3</sub> MnSb <sub>11</sub>	Yb <sub>13.61</sub> Gd <sub>0.40</sub> Mn <sub>1.11</sub> Sb <sub>11</sub> Yb <sub>13.57</sub> Gd <sub>0.40</sub> Mn <sub>1.11</sub> Sb <sub>11</sub>	Yb <sub>1</sub> Mn <sub>2.1</sub> Sb <sub>2</sub> Sn Yb <sub>1</sub> Mn <sub>2.1</sub> Sb <sub>2</sub> Sn
Yb <sub>13.5</sub> Gd <sub>0.5</sub> MnSb <sub>11</sub>	Yb <sub>13.50</sub> Gd <sub>0.49</sub> Mn <sub>1.11</sub> Sb <sub>11</sub> Yb <sub>13.47</sub> Gd <sub>0.49</sub> Mn <sub>1.10</sub> Sb <sub>11</sub>	Yb <sub>1</sub> Mn <sub>2.1</sub> Sb <sub>2</sub> Sn
Yb <sub>13.3</sub> Gd <sub>0.7</sub> MnSb <sub>11</sub>	Yb <sub>13.50</sub> Gd <sub>0.48</sub> Mn <sub>1.09</sub> Sb <sub>11</sub>	Yb <sub>1</sub> Mn <sub>2.1</sub> Sb <sub>2</sub>
Yb <sub>13.1</sub> Gd <sub>0.9</sub> MnSb <sub>11</sub>	Yb <sub>13.67</sub> Gd <sub>0.48</sub> Mn <sub>1.14</sub> Sb <sub>11</sub> Yb <sub>13.60</sub> Gd <sub>0.47</sub> Mn <sub>1.14</sub> Sb <sub>11</sub>	Yb <sub>1</sub> Mn <sub>2.1</sub> Sb <sub>2</sub> (Yb <sub>2</sub> Gd <sub>3</sub> )Sb <sub>5</sub>

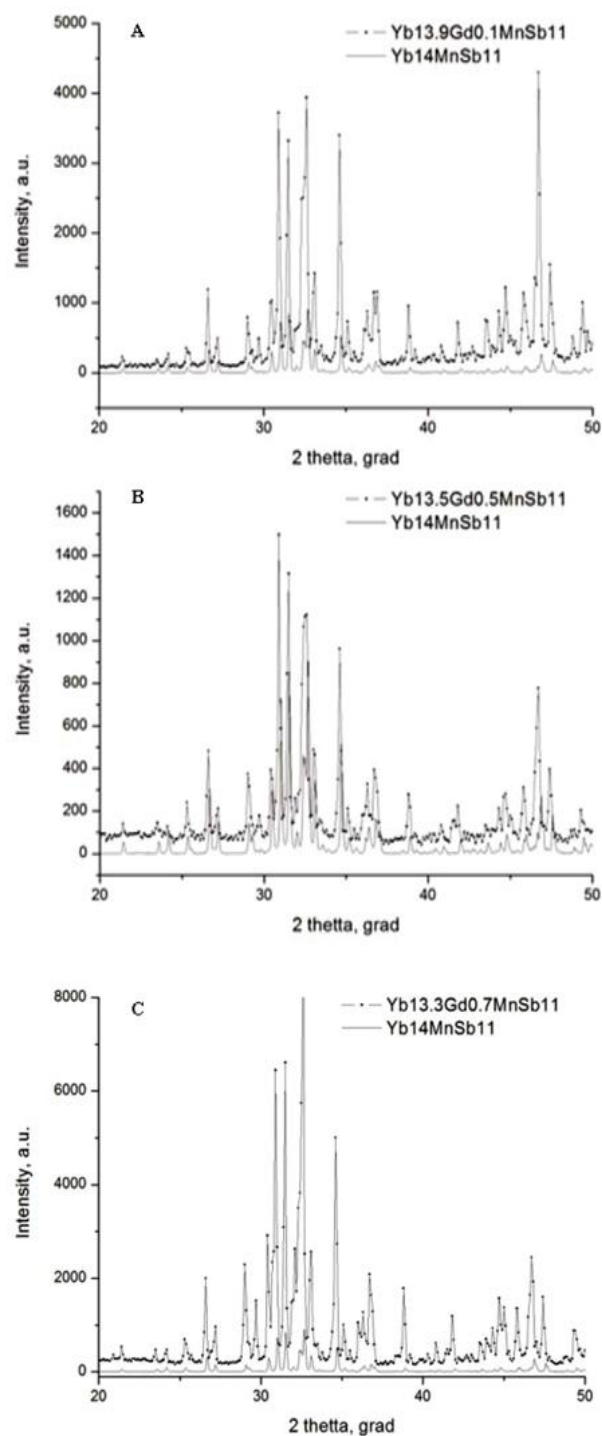


**Figure 1.** Power X-ray diffraction data for Yb<sub>13.9</sub>Gd<sub>0.1</sub>MnSb<sub>11</sub>(A), Yb<sub>13.5</sub>Gd<sub>0.5</sub>MnSb<sub>11</sub>(B) and Yb<sub>13.3</sub>Gd<sub>0.7</sub>MnSb<sub>11</sub>(C).

All crystals have tetragonal structure and these lattice parameters are given Table2.

**Table 2.** Structural data of the samples Yb<sub>14-x</sub>Gd<sub>x</sub>MnSb<sub>11</sub>.

Content Gd, x	a, Å	c, Å	V, Å <sup>3</sup>
0,1		22.000(11)	6075.47
0,3	16.624(8)	22.028(11)	6087.60
0,5	16.638(8)	22.055(11)	6105.33
0,7	16.639(8)	22.056(11)	6106.34
0,9*	16.636(8)	22.030(11)	6096.95

Thermo analysis found that compound Yb<sub>14</sub>MnSb<sub>11</sub> and their solid solutions is melt at high temperature. Obtained temperatures of melting are presented in the Table3.

**Table 3.** Some thermal properties of Yb<sub>14-x</sub>Gd<sub>x</sub>MnSb<sub>11</sub>.

Compounds	T <sub>melt</sub> , °C	α·10 <sup>-6</sup> , K <sup>-1</sup>	θ <sub>D</sub> , K
Yb <sub>14</sub> MnSb <sub>11</sub>	1745	13.0	167
Yb <sub>13,9</sub> Gd <sub>0,1</sub> MnSb <sub>11</sub>	1780	21.8	129
Yb <sub>13,7</sub> Gd <sub>0,3</sub> MnSb <sub>11</sub>	1790	17.4	144
Yb <sub>13,5</sub> Gd <sub>0,5</sub> MnSb <sub>11</sub>	1757	16.0	150
Yb <sub>13,3</sub> Gd <sub>0,7</sub> MnSb <sub>11</sub>	1796	20.0	135
Yb <sub>13,1</sub> Gd <sub>0,9</sub> MnSb <sub>11</sub>	1800	22.0	128

Investigation of thermal expansion determined that function ΔL/L<sub>0</sub>- f(T) is linear for all materials that indicate the constant coefficient of thermal dilatation α in this region of temperatures.

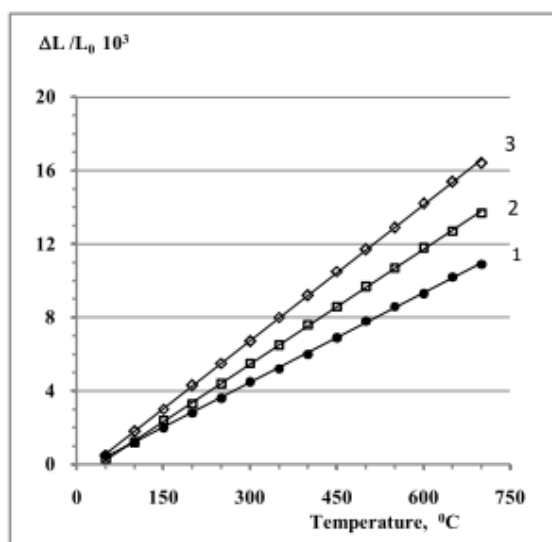


**Figure 2.** Determination ΔL/L<sub>0</sub>: 1 – Yb<sub>13,9</sub>Gd<sub>0,1</sub>MnSb<sub>11</sub>; 2 - Yb<sub>13,7</sub>Gd<sub>0,3</sub>MnSb<sub>11</sub>; 3 - Yb<sub>13,5</sub>Gd<sub>0,5</sub>MnSb<sub>11</sub>.

Thermal expansion coefficients presented in the table are found by slopes of straight lines.

To obtain information on chemical link stability characteristic temperature Debye and mean-square substitution in crystal were calculated.

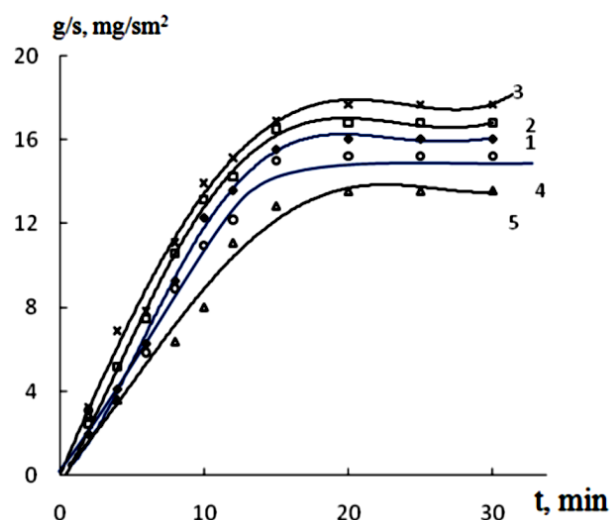
In [16], equation (1) which links thermal expansion coefficient with characteristic Debye temperature, was obtained by superposition of the Lindermann -Borelius and Grueneizen expressions:

$$\Theta_D = \frac{19.37}{\sqrt{\bar{A}} V^{2/3} \alpha} \quad (1)$$

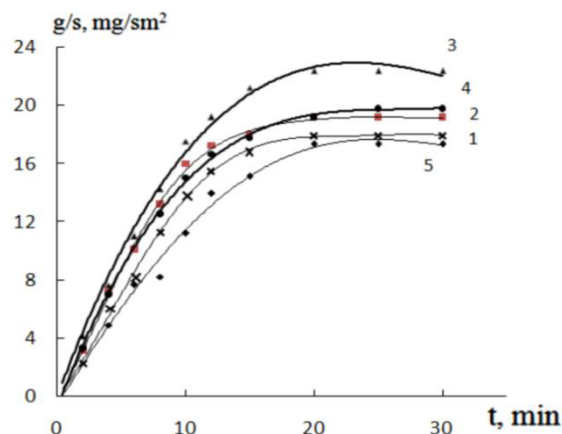
where  $\bar{A}$ - mean-square atomic weight; V- molecular volume; α- coefficient of thermal expansion.

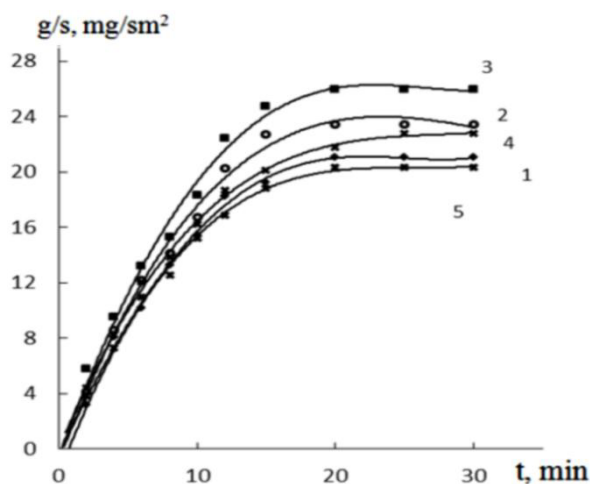
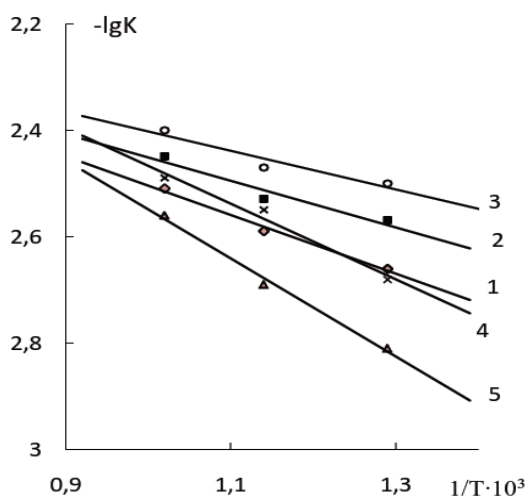
Both thermal expansion coefficients, melting temperatures and Debye temperatures evidences of changes after composition of gadolinium ≈ 0.5 characteristics. Probably it can be explained by that fact that solubility limit of gadolinium in this compound switches to this concentration.

The oxidation rate increases in all samples with the temperature increase. Oxidation curves have parabolic form with intensive oxidation rate in the initial period. In Figures 3-6 oxidation kinetic curves of solid solutions are presented. According to the kinetic curves built basing on change in sample weight depending on time, the oxidation rate was calculated at each temperature. True oxidation rate of the compounds calculated according to tangent, drawn from the coordinate start to the curves and calculated by formula:  $K = g/s \cdot \Delta t$ , is presented in Table4. According to the direct dependence  $\lg K - 1/T$ , apparent activation energy was calculated (Table4).



**Figure 3.** Kinetic curves oxidation Yb<sub>14-x</sub>Gd<sub>x</sub>MnSb<sub>11</sub> at 773K.



**Figure 4.** Kinetic curves oxidation  $\text{Yb}_{14-x}\text{Gd}_x\text{MnSb}_{11}$  at 873K.**Figure 5.** Kinetic curves oxidation  $\text{Yb}_{14-x}\text{Gd}_x\text{MnSb}_{11}$  at 973K.**Figure 6.** Dependence  $\lg K$  on  $1/T$  for  $\text{Yb}_{14-x}\text{Gd}_x\text{MnSb}_{11}$  with composition: 1-  $\text{Yb}_{13,9}\text{Gd}_{0,1}\text{MnSb}_{11}$ ; 2-  $\text{Yb}_{13,7}\text{Gd}_{0,3}\text{MnSb}_{11}$ ; 3-  $\text{Yb}_{13,5}\text{Gd}_{0,5}\text{MnSb}_{11}$ ; 4-  $\text{Yb}_{13,3}\text{Gd}_{0,7}\text{MnSb}_{11}$ ; 5-  $\text{Yb}_{13,1}\text{Gd}_{0,9}\text{MnSb}_{11}$ .**Table 4.** Kinetic and energetic parameters of oxidation alloys.

Solid solution compositions	Oxidation temperature, K	Oxidation rate, $\text{K} \cdot 10^{-4} \text{ kg/m}^2 \cdot \text{s}^{-1}$	Apparent activation energy, KJ/mol
$\text{Yb}_{13,9}\text{Gd}_{0,1}\text{MnSb}_{11}$	773	$0.22 \cdot 10^{-3}$	75.21
	873	$0.25 \cdot 10^{-3}$	
	973	$0.31 \cdot 10^{-3}$	
$\text{Yb}_{13,7}\text{Gd}_{0,3}\text{MnSb}_{11}$	773	$0.27 \cdot 10^{-3}$	62.7
	873	$0.29 \cdot 10^{-3}$	
	973	$0.36 \cdot 10^{-3}$	
$\text{Yb}_{13,5}\text{Gd}_{0,5}\text{MnSb}_{11}$	773	$0.31 \cdot 10^{-3}$	54.3
	873	$0.33 \cdot 10^{-3}$	
	973	$0.39 \cdot 10^{-3}$	
$\text{Yb}_{13,3}\text{Gd}_{0,7}\text{MnSb}_{11}$	773	$0.21 \cdot 10^{-3}$	91.96
	873	$0.27 \cdot 10^{-3}$	
	973	$0.33 \cdot 10^{-3}$	

$\text{Yb}_{13,1}\text{Gd}_{0,9}\text{MnSb}_{11}$	773	$0.15 \cdot 10^{-3}$	112.86
	873	$0.20 \cdot 10^{-3}$	
	973	$0.28 \cdot 10^{-3}$	

The maximum amount of each RE substituted for Yb was determined to be 0.7 for La, 0.6 for Ce, and 0.5 for Tm [5-8]. Microprobe analysis of the crystals of  $\text{Yb}_{14-x}\text{Gd}_x\text{MnSb}_{11}$  of which properties were measured provided the following compositions (Table 1) showing that the maximum amount of Gd that can substitute for Yb in  $\text{Yb}_{14-x}\text{Gd}_x\text{MnSb}_{11}$  is  $x = 0.48$ . As data show (Tables 2-4) maximum introduction of does not exceed  $x=0.5$ , that proves obtained values of melting temperature, coefficient of thermal expansion and activation energy.

Obtained physic-chemical characteristics along with another property allow us to assume the nature of this new class of inorganic materials.

## Acknowledgements

This work was supported by International Science & Technology Center (ISTC), #Project T-2067.

## References

- G.A. Slac, *CRC Handbook of Thermoelectrics* (CRC Press LLC, Boca Raton, FL, 1995)
- J. Y. Chan, M. M. Olmstead, S. M. Kauzlarich, D. J. Webb, *Chem. Mater.*, **10**, 3583 (1998)
- R. Fisher, T. A. Wiener, S. L. Bud'ko, P. C. Canfield, J. Y. Chan, S. M. Kauzlarich, *Phys. Rev.*, **B 59**, 13829 (1999)
- C. Yu, J. Zhu, S. H. Yang, J. J. Shen and X. B. Zhao, *Phys. Status Solid RRL*, **4**, 212 (2010)
- S. R. Brown, S. M. Kauzlarich, F. Gascoin, G. J. Snyder, *Chem. Mater.*, **18** (7), 1873 (2006)
- S. Kastbjerg, C. A. Uvarov, S. M. Kauzlarich, E. Nishibori, M. A. Spackman, B. Iversen, *Chem. Mater.*, **23** (16), 3723 (2011)
- B. C. Sales, P. Khalifah, T. P. Enck, E. J. Nagler, R. E. Sykora, R. Jin, and D. Mandrus, *Phys. Rev.*, **B 72**, 205207 (2005)
- J. H. Grebenkemper, S. M. Kauzlarich, *APL Mater.*, **3**, 0415031 (2015)
- C. A. Uvarov, M. Abdusalyamova, K. Star, J. – P. Fleurial and S. M. Kauzlarich, *Sci. Adv. Mater.*, **3**, 652 (2011)
- J. H. Roudebush, J. Grebenkemper, M. N. Abdusalyamova, S. M. Kauzlarich, *J. Sol. State Chem.*, **211**, 206 (2014)
- G. Yu, Y. Chen, H. Xie, G. Jeffrey, C. Fu, J. Fu, J. Xu, X. Zhao, T. Zhu, *J. Appl. Phys. Exp.*, **5**, 031801 (2012)
- E. S. Toberer, C. A. Cox, G. J. Snyder, S. R. Brown, T. Ikeda, S. M. Kauzlarich, A. F. May, *Trav. Adv. Func. Mater.*, **18**, 2785 (2008)
- J. F. Rauscher, C. A. Cox, T. Yi, C. H. Beavers, K. Klayins, E. S. Toberer, G. J. Snyder, S. M. Kauzlarich, *Dalt. Trans.*, **39**, 1055 (2010)
- T. Yi, P. Klavins, M. N. Abdusalyamova, F. Makhmudov, S. M. Kauzlarich, *J. Mater. Chem.*, **22**, 14378 (2012)

- 15 V. M. Glazov, N. N. Glagoleva, S. N. Chijievskay,  
*Liquid semiconductors*(Science, Moscow,1967)
- 16 N. N. Sirota, S. N. Chijievskay, *Physics and  
physicochemical analysis*(Science, Moscow, 1957)